Investigation on the abnormal quasi-two day wave activities during sudden stratospheric warming period of January 2006

Sheng-Yang Gu[1,2]*, Xiankang Dou[1,2,3], Dora Pancheva[4]

[1]CAS Key Laboratory of Geospace Environment, Department of Geophysics and Planetary Science, University of Science and Technology of China, Hefei, Anhui, China

[2]Mengcheng National Geophysical Observatory, School of Earth and Space Sciences, University of Science and Technology of China, Hefei, Anhui, China

[3]Wuhan University, Wuhan, China

[4]National Institute of Geophysics, Geodesy and Geography, BAS, Sofia, Bulgaria

*Corresponding Author: Sheng-Yang Gu (gsy@ustc.edu.cn)

Abstract

The quasi-two day wave (QTDW) during austral summer period usually coincides with sudden stratospheric warming (SSW) event in the winter hemisphere, while the influences of SSW on QTDW are not totally understood. In this work, the anomalous QTDW activities during the major SSW period of January 2006 are further investigated on the basis of hourly Navy Operational Global Atmospheric Prediction System-Advanced Level Physics High Altitude (NOGAPS-ALPHA) reanalysis dataset. Strong westward QTDW with zonal wave number 2 (W2) is identified following~~besides~~ the conventionally dominant mode of zonal wave number 3 (W3). Meanwhile, the W3 peaks with an extremely short period of ~42 hours. Compared with January 2005 with no evident SSW, we found that the zonal mean zonal wind in the summer mesosphere is enhanced during 2006. The enhanced summer easterly sustains critical layers for W2 and short-period W3 QTDWs with larger phase speed, which facilitate their amplification through wave-mean flow interaction. The stronger summer easterly also ~~provides stronger~~strengthens the barotropic/baroclinic instabilities and thus provides larger forcing for the amplification of QTDW. The inter-hemispheric coupling~~ induced by strong winter stratospheric planetary wave activities~~ during SSW period is most likely responsible for the enhancement of summer easterly. Besides, we found that the nonlinear interaction between W3 QTDW and the wave number 1 stationary planetary wave (SPW1) ~~may also contribute to the source of W2~~most possibly occur at middle and low latitudes in the mesosphere. We conclude that the abnormal QTDW behaviors during January 2006

are intimately correlated to the major SSW event during the same time.

1. Introduction

The temperature and wind fields in the mesopause region exhibit significant variability~~strong oscillation~~ with ~~a~~ the period of several days, of which the Quasi-Two-Day wave (QTDW) is the most frequently reported planetary wave (*Palo et al.*, 2007; *Limpasuvan and Wu*, 2009; *McCormack et al.*, 2009; *Pedatella and Forbes*, 2012; *Yue et al.*, 2012; *Chang et al.*, 2014; *Siskind and McCormack*, 2014; *Guharay et al.*, 2015; *Lilienthal and Jacobi*, 2015; *Madhavi et al.*, 2015; *Gu et al.*, 2016a; *Pancheva et al.*, 2016; *Wang et al.*, 2017). There are both eastward and westward QTDWs with different zonal wave numbers, including the westward modes with zonal wave numbers 2 (W2), 3 (W3) and 4 (W4), and the eastward modes with zonal wave numbers 2 (E2) and 3 (E3) (*McCormack et al.*, 2014; *Gu et al.*, 2016b; *Pancheva et al.*, 2016). The eastward QTDWs are usually found ~~to exist~~ in the winter hemisphere (*Sandford et al.*, 2008; *Gu et al.*, 2017), while the westward modes tend to be summer phenomena that peak shortly after the solstice (*Pancheva et al.*, 2004; *Tunbridge et al.*, 2011). In the southern hemisphere, the westward QTDWs show maximum amplitude during January/February at middle and low latitudes (*Limpasuvan and Wu*, 2003; *Palo et al.*, 2007; *Gu et al.*, 2013a). In the northern hemisphere, the QTDW peaks intermittently from June to August at middle latitudes (*McCormack et al.*, 2014; *Gu et al.*, 2016b; *Pancheva et al.*, 2016). Generally, the QTDW activities during the austral summer period are much stronger than those during boreal summer period and thus have received more attention (*Gu et al.*, 2013a; *Pancheva et al.*, 2016; *Tunbridge et al.*, 2011).

The propagation and amplification of planetary waves are intimately related to the background zonal wind (*Gu et al.*, 2016b; *Liu et al.*, 2004; *Yue et al.*, 2012). As for the QTDW, it has been shown that the baroclinic/barotropic instability of the summer easterly jet is an important source for its amplification (*Chang et al.*, 2011; *Yue et al.*, 2012). The Eliassen-Palm (EP) flux associated with QTDW grows dramatically near its critical layer (where the background wind equals its phase speed), which indicates the energy transportation from mean flow. The Advanced Level Physics High Altitude version of the Navy Operational Global Atmospheric Prediction System (NOGAPS-ALPHA) reanalysis dataset shows that the inter-annual variations of the QTDW during boreal summer period are dependent on the strength of the summer easterly. A stronger summer easterly provides larger forcing for its amplification (*McCormack et al.*, 2014). Recently, *Gu et al.* (2016a) found that the strength of the summer easterly is also responsible for the selective amplification of QTDWs with different zonal wave numbers. The ~~westward zonal wave number 2 (~~W2~~)~~ QTDW peaks with a stronger summer easterly than the ~~westward zonal wave number 3 (~~W3~~)~~ mode. This is because a stronger summer easterly can sustain a critical layer for QTDW with larger phase speed (e.g., W2), and the amplification of QTDW occurs more easily at the unstable region with a critical layer (*Liu et al.*, 2004; *McCormack et al.*, 2014).

Sudden Stratospheric Warmings (SSWs) occur in the winter stratosphere, and are most frequently observed during boreal winter period (December-February). The zonal mean temperature at 10 hPa and 60^{o}N can increase by tens of Kelvin in one or two weeks during a SSW event. It is called a major SSW if the westerly wind at 10 hPa and 60°N reverses, while the winter westerly is slowed down but does not become easterly during a minor SSW. It is generally accepted that the westward forcing from the rapid amplification of planetary waves is responsible for the wind deceleration or reversal in the winter stratosphere (*Matsuno*, 1971; *Liu and Roble*, 2002). Interestingly, the occurrence of SSW in the northern hemisphere winter stratosphere usually coincides with the temporal variation of the QTDW in the summer mesosphere. Nevertheless, their influence on each other has not been totally understood yet.

Evidence has been found for inter-hemispheric coupling during a SSW event, which may have significant modulation on summer easterly jet and thus the amplification of planetary waves. *Karlsson et al.* (2007) showed that the noctilucent cloud in the summer mesosphere has an inverse relationship with the temperature variations in the winter stratosphere. Further correlation analysis confirmed that the dynamics in the winter stratosphere does have global influence on the atmospheric mean state (*Karlsson et al.*, 2009; *Körnich and Becker*, 2010; *Tan et al.*, 2012). The feedback between gravity-wave drag and zonal wind induced by mesospheric cross-equatorial flow is a reasonable explanation for the inter-hemispheric coupling mechanism. *Stray et al.* (2015) proposed that the enhancement of wave number 1 and 2 planetary waves at ~95 km could be a common feature during SSW period. Thus it is reasonable to argue that the SSW may also have significant influence on QTDW (*Lima et al.*, 2012). It has been illustrated that the stratospheric ozone depletion in southern hemisphere spring (September-November) can also result in enhanced instabilities in the mesosphere, which contributes to the growth of mesospheric planetary wave activities (*Lossow et al.*, 2012; *Lubis et al.*, 2016). Nevertheless, we should note that the QTDW is a summer phenomenon that usually occurs in January or February. Thus the enhanced instability induced by ozone depletion may be ineffective for the amplification of QTDW.

A strong SSW event occurred in January 2006, when the QTDW activities also exhibited abnormal behaviors consisting of an unusually strong W2 QTDW identified in the wind and temperature fields besides the conventional W3 mode (*Varavut Limpasuvan and Wu*, 2009). Meanwhile the W3 QTDW peaks with an extremely short period of ~42 hours (*Gu et al.*, 2013a, b). It was suggested that these abnormal QTDW activities may be related to the unusually strong summer easterly during the same period. *McCormack et al.* (2009) proposed that the strong planetary waves leading to the SSW event could influence the background zonal wind and the QTDW forcing by enhancing the northward component of the residual circulation. This theory was supported by simulations from the control thermosphere-ionosphere-mesosphere-electrodynamics general circulation model (TIME-GCM), which show that the zonal mean zonal wind and the mean flow instability become stronger during a SSW event (*Gu et al.*, 2016c). Besides, they also reported the nonlinear interaction between W3 QTDW and the zonal wavenumber 1 stationary planetary wave (SPW1), which generates a W2 QTDW (*Gu et al.*, 2015). Nevertheless, unrealistic QTDW and SPW1 forcing is utilized in their numerical simulation to compensate strong dissipation at lower model boundary (~10 hPa), which may result in artificial nonlinear coupling. Thus, the influence of SSW on QTDW needs further investigation with more realistic atmospheric conditions.

In addition to ground-based and satellite observations, synoptic meteorological datasets could be utilized to perform diagnostic analysis on the propagation and amplification of QTDW. In this paper, the anomalous QTDW activities during the major SSW period of January/February 2006 will be further investigated on the basis of NOGAPS-ALPHA reanalysis dataset, which has been proven to be capable of reproducing both SSW and QTDW activities under realistic atmospheric conditions (*McCormack et al.*, 2009). This work sheds new light on the question whether or not the SSW in the winter stratosphere has significant influence on the QTDW in the summer mesosphere. The dataset and analysis are briefly described in section 2. Our analysis results are presented in section 3, followed by a summary in section 4.

2. Datasets and analysis

2.1 Aura/MLS temperature

The Aura satellite was launched on July 15, 2004, which is a major component of the NASA Earth Observing System (EOS). The Microwave Limb Sounder (MLS) is one of the four instruments onboard the Aura satellite that measures emissions from ozone, chlorine and other trace gases with a sun-synchronous orbit (covering two local times at a given latitude from ~82ºS-82ºN) (Schwartz et al., 2008). Aura satellite travels around the earth with a period of ~99 minutes, and thus the atmosphere is sampled with ~14.5 circles per day. The version 3.3 Aura/MLS temperature dataset ranges from 261 hPa to 0.001 hPa (~10-96 km) with a precision of 0.6 K in the lower stratosphere and 2.5 K in the mesosphere. The highest vertical resolute of 3.6 km lies at 31.6 hPa, which degrades to ~6 km at 0.01 hPa. A least squares fitting method is utilized to extract the QTDW information in Aura/MLS temperature from December 2005 to February 2006, which is then compared with the results from NOGAPS-ALPHS reanalysis dataset.

2.2 NOGAPS-ALPHA

The NOGAPS-ALPHA reanalysis model is developed at Naval Research Laboratory (NRL), which is the Advanced Level Physics High Altitude version of the Navy Operational Global Atmospheric Prediction System. The NRL Atmospheric Variational Data Assimilation System (NAVDAS) is adopted to incorporate both ground-based and satellite observations (*Daley and Barker*, 2001), including the global temperature observations from Aura/MLS and TIMED/SABER instruments. The observational datasets are updated every 6 hours through the NAVDAS. Nevertheless, we use the hourly meteorological fields from NOGAPS-ALPHA to study the QTDWs. Please refer to *Eckermann et al.* (2009) and *Siskind et al.* (2012) for more information about the model and data assimilation.

The NOGAPS-ALPHA reanalysis datasets have been previously used to study atmospheric tides and QTDWs. For example, *Lieberman et al.* (2015) studied the short-term variability of the nonmigrating tide and its relationship with the nonlinear interaction between stationary planetary wave and migrating tide. *Pancheva et al.* (2016) analyzed the global distribution and seasonal variation of both eastward and westward propagating QTDWs. In addition, the inter-annual variability of the nonlinear interactions between QTDW and migrating diurnal tide has also been investigated (*McCormack et al.*, 2010; *McCormack et al.*, 2014). Their analysis results show that the NOGAPS-ALPHA reanalysis model is capable of capturing tidal and planetary wave behaviors in the atmosphere. We will use a two-dimensional least squares fitting to extract QTDW signals in the NOGAPS-ALPHA dataset.

3. Results and Discussion

3.1 QTDWs in Aura/MLS temperature

Figures 1a and 1c show the spectra of the Aura/MLS temperature observation at ~0.005 hPa during January 12-19 and 23-30 of 2006, when the W3 and W2 reach maximum amplitudes (shown later by Figure 2). The MLS observations at ~40ºS and ~20ºS are utilized in Figures 1a and 1c, respectively. It is clear that the W3 and W2 QTDWs dominate the wave spectra with periods of ~42 and ~45 hours, respectively. The vertical and global structures of the W3 and W2 are shown in Figures 1b and 1d. Most of the W3 oscillations are limited to the southern hemisphere with maximum amplitude of ~12 K at ~~~40ºN~~ 40ºS and 0.005 hPa. The temperature field of W2 exhibits comparable perturbations in both hemispheres, though the branch in the southern hemisphere is slightly stronger than that in the northern hemisphere. This is because the larger phase speed of W2 results in more broadly distributed ~~positive~~ refractive index, which enables its propagation in both hemispheres (*Liu et al.*, 2004; *Gu et al.*, 2016c). The temporal variations of the QTDWs in the summer mesosphere and the zonal mean temperature anomaly in winter stratosphere are plotted in Figure 2. The W3 QTDW grows as the development of SSW in early January, and reaches maximum amplitude at around January 15. The W2 QTDW reaches maximum amplitude of ~6 K at around January 27 with a minor peak of ~3 K at around January 10. Both the W2 and W3 QTDWs fade away after February 9, when the SSW also disappears and the atmosphere returns to a climatological state. Figure 3 shows the comparison between the QTDWs during 2005 and 2006. Abnormally strong W2 activities are observed during January 2006, which are very weak during January 2005. Besides, the W3 QTDW is also stronger in January 2006. These QTDW activities agree well with the results presented by *Limpasuvan and Wu* (2009) and *Tunbridge et al.* (2011). We will then investigate whether the abnormal QTDW activities during January 2006 are related to the major SSW event during the same episode with NOGAPS-ALPHA reanalysis dataset.

3.2 QTDWs in NOGAPS-ALPHA

Figure 4 shows the analysis results of W2 and W3 from NOGAPS-ALPHA during the same time period as Figure 1. The W3 and W2 QTDW signals are also clearly indicated in the NOGAPS-ALPHA reanalysis datasets, and their vertical and latitudinal temperature structures agree well with the results from Aura/MLS. Besides, we found that the temporal variations of both W2 and W3 (Figure 5) are also consistent with Aura/MLS observations (Figure 2). This is not strange since the Aura/MLS and TIMED/SABER temperature datasets are major components incorporated in the data assimilation at mesopause. We will also compare the wind structures of QTDW from NOGAPS-ALPHA with those in previous literatures. Figure 6 shows the zonal and meridional wind structures of W2 and W3 in NOGAPS-ALPHA. The perturbations of W3 are nearly twice as strong as the W2.

Again, we can see that the latitudinal structures of W2 are more symmetric to the equator than W3. The zonal and meridional winds of W3 peak in the southern hemisphere with amplitudes of ~45 m/s and ~65 m/s at ~50ºS and ~40ºS, respectively. The zonal wind of W2 peaks at ~20º-40º in both hemispheres with amplitudes of ~10-20 m/s, while the meridional wind of W2 maximizes at the equator with amplitude of ~35-40 m/s. Generally, these results agree well with previous satellite observations (*Limpasuvan and Wu*, 2009; *Gu et al.*, 2013a). Thus we conclude that both the temperature and wind fields in NOGAPS-ALPHA are reasonable and comparable with realistic atmospheric state, which can be utilized in ~~the mechanical~~ studying ~~of~~ the anomalous QTDW activities during January 2006.

It is proposed that the SSW may have significant influence on QTDW by changing the mean flow (*Gu et al.*, 2016c). Thus we will first show how the background wind influences the amplification of QTDWs. A necessary condition for the occurrence of baroclinic/barotropic instability for zonal mean zonal wind is $\bar{q}_{\varphi} < 0$, where $\bar{q}_{\varphi}$ is the latitudinal gradient of the quasi-geostrophic potential vorticity (*Liu et al.*, 2004):

$$\bar{q}_{\varphi} = 2\Omega\cos\varphi - \left(\frac{(\bar{u}\cos\varphi)_{\varphi}}{a\cos\varphi}\right)_{\varphi} - \frac{a}{\rho}\left(\frac{f^2}{N^2}\rho\bar{u}_z\right)_z \qquad (1)$$

where $\bar{u}$, a, φ, f, N, Ω, and ρ are the zonal mean zonal wind, earth radius, latitude, Coriolis parameter, Brunt-Väisällä frequency, angular speed of the earth's rotation, and the background air density, z means the vertical gradient. The second and third parts of the equation on the right denote barotropic and baroclinic instabilities induced by the latitudinal and vertical gradients of the zonal mean zonal wind, respectively.

Planetary waves can be amplified by the instabilities through mean-flow interaction. It has been found that the EP flux of QTDW grows dramatically after the over-reflection by its critical layer (where the zonal mean zonal wind equals to the planetary wave speed) near the unstable region (*Liu et al.*, 2004). The EP flux of planetary waves, (e.g., QTDW), can be calculated following *McCormack et al.* (2014):

$$\vec{F}_{EP} = \rho a \cos\varphi \begin{bmatrix} -\overline{v' u'} \\ \left[f - \dfrac{(\bar{u}\cos\varphi)_{\varphi}}{a\cos\varphi} \right] \dfrac{\overline{v'\theta'}}{\bar{\theta}_z} \end{bmatrix} \qquad (2)$$

where *u*', *v*', and *θ*' are the zonal wind, meridional wind, and potential temperature perturbations of planetary waves. The phase speed of planetary wave can be calculated by $(2\pi \cdot a)/(s \cdot T)$, where the *s* and T are the zonal wave number and period, respectively.

The barotropic/baroclinic instabilities of the mean flow and the EP flux of W2 and W3 are shown in Figure 7. It is clear that the W3 is more favorable to propagate in the summer hemisphere, and is dramatically amplified by the mean flow instabilities at middle latitude between 0.1 and 0.01 hPa. Nevertheless, the W2 is capable of propagating in both hemispheres due to its more broadly distributed refractive index (*Gu et al.*, 2016c), which is also shown by Figure 8. The summer branch is also amplified by the instabilities related to the easterly wind, while the winter branch propagates directly from the lower atmosphere to mesosphere. *Liu et al.* (2004) has shown that the amplification of QTDW through wave-mean flow interaction most easily occurs near its critical layer, which is also indicated in our analysis. Compared with W3 QTDW, which is more obviously amplified by the mean instabilities, the W2 QTDW looks more like a free traveling planetary wave. There are only very weak clues at 20-40ºS and 0.1-0.01 hPa showing the outflow of W2 EP flux from the instability region. This may be also due to the larger phase speed of W2, which make W2 less vulnerable to mean wind dissipations and travel more freely when propagating upward. To better quantitatively investigate the role of barotropic and baroclinic instabilities, Figure 9 shows the barotropic and baroclinic instabilities separately. We found that the barotropic instability is usually ~60-80% as strong as the baroclinic instability at middle latitudes in the summer mesosphere, where it is more effective for the amplification of QTDW. In other words, the wind vertical shears generally contribute more to the growth of QTDW, but the wind curvatures are also very important.

Figure 2 has shown that both the QTDWs and the SSW peak in the middle and late January, thus Figure ~~8~~ 10 shows the comparison between the zonal mean zonal wind during January 11-30 of 2005 and 2006. The zonal wind during the SSW period of 2006 shows two major differences compared with that in 2005. First, the westerly wind in winter stratosphere reverses to easterly. The winter westerly reversal is one key feature of major SSW, which is induced by the rapid growth of stationary planetary waves and their momentum deposition to the background mean flow (*Liu and Roble*, 2002). Second, the summer easterly wind in the mesosphere is enhanced. The interhemispheric couplings during SSW period have been reported in previous literatures (*Karlsson et al.*, 2007, 2009; *Körnich and Becker*, 2010). We then analyzed the correlation between the temporal variations of the global zonal mean zonal wind and the zonal mean temperature at 70ºN and 10 hPa, which increase dramatically during a SSW event. The correlation coefficients are shown in Figure ~~9~~11. The zonal wind in the summer mesosphere at middle latitude shows a significant inverse relationship with the temperature variations in the winter stratosphere. In the summer hemisphere, the zonal mean zonal wind is westward in the upper stratosphere and mesosphere; it will be enhanced when the temperature in winter stratosphere increases. The SSW is mainly caused by the rapid growth of planetary waves, which deposits energy and momentum flux to the background wind. Figure 12 shows the zonal mean circulations induced by the momentum flux of SPW1, which is calculated using the downward control principle following *Haynes et al.* (1991) and *Lubis et al.* (2016). It is clear that the SPW1 induced zonal mean circulation shows maxima in winter polar stratosphere with amplitudes of -6-7 cm/s (downward) and 7-8 m/s (northward) for vertical and meridional components, respectively. It is also clear that the SPW1 induced circulations are confined to the winter hemispheres, and thus contribute little to the inter-hemispheric coupling. This agrees well with the mechanism that the inter-hemispheric coupling is induced by the feedback between gravity wave breaking and zonal mean zonal wind in the mesosphere (*Karlsson et al.*, 2009; *Körnich and Becker*, 2010). Figure 13 shows the differences between the meridional circulation during and before the SSW following *Lubis et al.* (2016), which clearly indicates an anomalous cross-equator circulation from the winter to summer mesosphere. Thus, we conclude that the zonal wind anomaly during January 2006 is most likely correlated with the SSW event.

We then show how these differences result in different QTDW behaviors during 2005 and 2006. The mean flow instabilities of the background wind and the critical layers of W2 and W3 are shown in Figure ~~10~~14. First the enhanced summer easterly in the mesosphere results in stronger barotropic/baroclinic instability, which provides larger forcing for the amplification of QTDW. This results in stronger W3 amplitude during 2006 than that during 2005 (Figure 3). Besides, the stronger summer easterly in the mesosphere also sustains a critical layer for W2 during 2006 at middle latitude, which is not observed in 2005. The phase speed of planetary wave is inversely proportional to both period and zonal wave numbers, thus the phase speed of W2 is larger than W3. The existence of W2 critical layer nearby the instability region facilitates the wave-mean flow interaction, through which the energy of mean flow is transferred to W2 (*Liu et al.*, 2004). This results in abnormally strong W2 oscillations in 2006 than that in 2005. *Gu et al.* (2013b) also noted that the W3 during 2006 peaks with an extremely short period of ~42 hours (also shown by Figure 1 and 4), whereas the period of W3 during austral summer tends to be longer (~52 hours) (*Palo et al.*, 2007; *Tunbridge et al.*, 2011; *Yue et al.*, 2012). The W3 QTDW with a longer period has a slower phase speed. Figure ~~11~~ 15 shows the comparison between the critical layers of 42- and 52-hour W3 for the zonal mean state during 2006. The critical layer of the 42-hour W3 runs at the edge of the mean flow instability, which is totally surrounded by the critical layer of the 52-hour W3. Thus the 52-hour QTDW signal has already been reflected away by the critical layer before it reaches the unstable region and cannot be amplified through wave-mean flow interaction (*Liu et al.*, 2004).

Figure ~~10b~~ 14b also shows that both the critical layers of W3 and W2 run across the mean flow instabilities in winter stratospheric region, whereas there is no significant positive EP flux divergence near this region (Figure ~~12~~16) as that shown in the summer mesosphere. Positive EP flux divergence indicates the energy conversion to planetary waves from mean flow instability (Liu et al., 2004).~~source for planetary waves.~~ Thus we conclude that the mean flow instability related to the winter westerly reversal during SSW period is not as effective for the QTDW amplification as that in the summer mesosphere.

3.3 The nonlinear coupling between W3 and SPW1

In the TIME-GCM numerical simulations, *Gu et al.* (2015) found that the W2 peaks earlier than W3 due to the fact that the W2 has a larger phase speed and thus suffers weaker dissipation during its propagation and amplfication. We should also note that the W2 is emmediately geneated through the nonlinear interaction, when the W3 and SPW1 are forced simutaneously at the lower model boundary. However, we found that the W2 peaks later than W3 duirng January 2006, which suggest a later occurrence of the nonlinear interaction. ~~*Gu et al.* (2015) proposed that the nonlinear interaction between W3 and SPW1 could also provide sources for W2.~~ We also calculated the nonlinear advection between W3 and SPW1 following *Gu et al.* (2016c) as a substitute to represent their nonlinear interaction:

$$F_{nonlinear,y} = -\frac{1}{a\cos\varphi}\left(u_1\frac{\partial v_2}{\partial\lambda} + u_2\frac{\partial v_1}{\partial\lambda}\right) - \frac{1}{a}\left(v_1\frac{\partial v_2}{\partial\varphi} + v_2\frac{\partial v_1}{\partial\varphi}\right) \quad (3)$$

The meridional nonlinear advection~~which~~ is shown in Figure ~~13~~17. The nonlinear advection from TIME-GCM shows a significant peak at the lower boundary (~10 hPa) in the winter stratosphere (Figure 13 of *Gu et al.* (2016c)), which is not shown by our results from NOGAPS-ALPHA. Note that both the W3 and SPW1 is forced at the lower model boundary in TIME-GCM (~10 hPa), which is much stronger than realistic situation to compensate the large dissipation. Thus we conclude that the nonlinear advection between W3 and SPW1 is in fact insignificant in the winter stratosphere. Besides, the nonlinear advection also shows four peaks in the mesosphere. The peak in polar winter mesosphere (~85ºN, 0.01 hPa) is most possibly related to the strong wave number 1 component of the wind oscillations, which is shown by Figure ~~14~~18. Considering that the W2 is only favored to propagate at middle and low latitudes (*Gu et al.*, 2016c), the nonlinear coupling between W3 and SPW1 in the winter polar region maybe ineffective for the observed W2 perturbations. There are both significant wind perturbations for W3 and SPW1 at low latitudes in the northern hemisphere (Figure ~~14~~18), and their nonlinear advection reaches ~12-15 m/s/day in this region. This agrees well with the result from TIME-GCM and possibly contributes to the northern branch of W2 (Figure 7b). The EP flux divergence of W2 in Figure ~~12~~ 16 also shows a source at ~10ºN between 0.01 and 0.001 hPa, which is possibly related to the nonlinear advection between W3 and SPW1. The wind perturbations of W3 reach maximum amplitude at middle and low latitudes in the summer mesosphere, and the nonlinear advection also reaches ~15 m/s/day and ~9 m/s/day at ~50ºS and ~10ºS, respectively. These nonlinear couplings may contribute to the southern branch of W2 (Figure 7b) and its positive EP flux divergence at ~25ºS between 0.01 and 0.001 hPa (Figure ~~12a~~16a).

Though the W3 and SPW1 shows significant nonlinear coupling at middle and low latitudes in the mesosphere, this does not mean that the nonlinear interaction is the only source for W2. The EP flux of W2 in the winter stratosphere shows clear upward propagation tendency, which most probably originates from the lower atmosphere (Figure ~~15~~19). The strong planetary wave activity in winter hemisphere, which is responsible for the occurrence of SSW, may also provide strong sources for QTDW in the lower atmosphere. *Gu et al.* (2016a, b) also showed that there are persistent QTDW signals in the lower atmosphere, whereas the amplification of QTDW in the mesosphere is dependent on the strength of the summer easterly. The interhemispheric coupling during SSW period results in strong summer easterly jet in January 2006, which provides suitable condition for the amplification of W2 signals in the lower hemisphere.

4. Discussion and Summary

~~In this paper, the influence of SSW on QTDWs is further investigated with NOGAPS-ALPHA reanalysis dataset, which is a further contribution to previous work reported by *Gu et al.* (2016c). Their TIME-GCM simulations use a climatological atmosphere state as the background and the planetary waves are forced at the lower model boundary (~10 hPa), which may induce artificial signals. Nevertheless, the NOGAPS-ALPHA reanalysis dataset incorporates realistic observation from the ground to mesosphere, which avoids the lower boundary effect. Our analysis shows that the nonlinear interaction between W3 and SPW1 most probably occurs at middle and low latitudes in the mesosphere.~~

Usually, the west zonal wave number 3 mode dominates the QTDW oscillations during austral summer periods, whereas~~During the major SSW period of January 2006,~~ the QTDWs exhibit strong oscillations with both zonal wave number 2 and 3 during the major SSW period of January 2006 (*Limpasuvan and Wu*, 2009). Besides,~~and~~ we found that the conventional wave number 3 mode peaks at an extremely short period according to previous statistics. Diagnostic analysis shows that the anomalous QTDW behaviors are related to the enhanced summer easterly.~~We found that the inter-hemispheric coupling induced by strong winter planetary wave activities plays a crucial role in connecting the winter stratospheric SSW and the summer mesospheric QTDW. To be exact, the summer easterly is enhanced during a SSW event through the inter-hemispheric coupling, which results in anomalous QTDW behaviors.~~ To be exact, ~~T~~the enhanced summer easterly can sustain critical layers for QTDW with larger phase speed (e.g., smaller zonal wave number, short period), which facilitate their amplification through wave-mean flow interactions. Moreover, the enhanced summer easterly also provides stronger barotropic/baroclinic instabilities and thus a larger forcing for the amplification of QTDW, which results in strong W3 oscillation during January 2006.

According to the mechanisms proposed by *Karlsson et al.* [2009] and *Körnich and Becker* [2010], the enhancement of summer easterly is most probably related to the major SSW in the winter hemisphere through inter-hemispheric couplings. The feedback between gravity wave breaking and zonal mean state may induce a trans-equator meridional circulation from the winter to summer mesosphere [*Körnich and Becker*, 2010], and this is confirmed by our analysis on the meridional circulation during January 2006. Our calculation also shows that the winter planetary wave induced variations in zonal mean circulation are confined to the winter hemisphere, which is less effective for the inter-hemispheric couplings. This, on the contrary, indicates the importance of gravity waves during the inter-hemispheric coupling. The meridional circulation anomaly induced by the variation of gravity wave drag during SSW period needs our further investigation in the future, since the gravity parameter is not included in the publicly accessed NOGAPS-ALPHA reanalysis dataset.

Gu et al. (2016c) studied the influence of SSW on QTDWs with TIME-GCM simulations. Their TIME-GCM simulations used a climatological atmosphere state as the background and the planetary waves are forced at the lower model boundary (~10 hPa), which may induce artificial signals. Nevertheless, the present NOGAPS-ALPHA reanalysis dataset incorporates realistic observation from the ground to mesosphere, and also avoids the lower boundary effect. For example, the TIME-GCM simulation shows strong nonlinear advection at the lower boundary (~10 hPa), which is not exhibited by NOGAPS-ALPHA. In other words, the enhanced nonlinear advection at ~10 hPa is most possibly due to the larger wave perturbations forced at the lower model boundary, and the nonlinear interaction between W3 and SPW1 most probably occurs at middle and low latitudes in the northern mesosphere. Besides, the W2 QTDW peaks earlier than the W3 QTDW in TIME-GCM simulations. This is due to that the W3 and W2 QTDWs are generated nearly simultaneously in TIME-GCM, and the W2 is less vulnerable to atmospheric dissipation due to its larger phase speed. Nevertheless, the W2 may maximize later than W3 according to the occurrence time of the nonlinear interaction, such as the situation during January 2006. In addition, the W3 QTDW becomes weaker during SSW period due to the nonlinear interaction and energy transfer from W3 to W2 in previous TIME-GCM simulations, where a constant forcing of W3 is added. However, the W2 and W3 QTDWs could be both strong in real atmosphere due to the strong winter planetary wave activities during SSW period, which could contribute to the source of QTDWs in the lower atmosphere. It is thus suggested that the current analysis with NOGAPS-ALPHA reanalysis dataset is a further contribution to the previous work with theoretical numerical simulation.

~~Thus, w~~We conclude that the abnormal QTDW activities in the summer mesosphere observed by *Limpasuvan and Wu* (2009) are correlated ~~with~~ to the major SSW event in the winter stratosphere through inter-hemispheric coupling. We should note that the summer easterly may also exhibit~~s~~ strong inter-annual variations, which could result in different QTDW activities during other SSW years. A detailed comparison between the QTDWs (with different zonal wave numbers) during SSW and non-SSW years will be statistically studied in the future.

Acknowledgement

This work is sponsored by the Project Funded by China Postdoctoral Science Foundation (2015M582001, 2016T90573), the National Natural Science Foundation of China (41421063, 41304123), and Hundred Talents Program (D). The NOGAPS-ALPHA dataset is available at ftp://map.nrl.navy.mil/pub/nrl/nogaps and the Aura/MLS temperature observation can be downloaded by

https://acdisc.gesdisc.eosdis.nasa.gov/data/Aura_MLS_Level2/.~~https://disc.sci.gsfc.nasa.gov/Aura/data-holdings/MLS.~~

References

Chang, L. C., S. E. Palo, and H. L. Liu (2011), Short-term variability in the migrating diurnal tide caused by interactions with the quasi 2 day wave, *Journal of Geophysical Research-Atmospheres*, *116*.

Chang, L. C., J. Yue, W. Wang, Q. Wu, and R. R. Meier (2014), Quasi two day wave-related variability in the background dynamics and composition of the mesosphere/thermosphere and the ionosphere, *Journal of Geophysical Research: Space Physics*, *119*(6), 4786-4804.

Daley, R., and E. Barker (2001), NAVDAS: Formulation and diagnostics, *Mon Weather Rev*, *129*(4), 869-883.

Eckermann, S. D., et al. (2009), High-altitude data assimilation system experiments for the northern summer mesosphere season of 2007, *Journal of Atmospheric and Solar-Terrestrial Physics*, *71*(3-4), 531-551.

Gu, S.-Y., H.-L. Liu, N. M. Pedatella, X. Dou, and Z. Shu (2016a), The quasi-2 day wave activities during 2007 boreal summer period as revealed by Whole Atmosphere Community Climate Model, *Journal of Geophysical Research: Space Physics*, *121*(7), 7256-7268.

Gu, S.-Y., H.-L. Liu, N. M. Pedatella, X. Dou, T. Li, and T. Chen (2016b), The quasi 2 day wave activities during 2007 austral summer period as revealed by Whole Atmosphere Community Climate Model, *Journal of Geophysical Research: Space Physics*, *121*(3), 2743-2754.

Gu, S.-Y., H.-L. Liu, N. M. Pedatella, X. Dou, and Y. Liu (2017), On the wave number 2 eastward propagating quasi 2 day wave at middle and high latitudes, J.

Geophys. Res. Space Physics, 122, 4489–4499, doi:10.1002/2016JA023353.

Gu, S.-Y., H.-L. Liu, T. Li, X. Dou, Q. Wu, and J. M. Russell (2015), Evidence of nonlinear interaction between quasi 2 day wave and quasi-stationary wave, *Journal of Geophysical Research: Space Physics*, *120*(2), 1256-1263.

Gu, S. Y., H. L. Liu, X. Dou, and T. Li (2016c), Influence of the sudden stratospheric warming on quasi-2-day waves, *Atmos. Chem. Phys.*, *16*(8), 4885-4896.

Gu, S. Y., T. Li, X. K. Dou, Q. Wu, M. G. Mlynczak, and J. M. Russell (2013a), Observations of Quasi-Two-Day wave by TIMED/SABER and TIMED/TIDI, *Journal of Geophysical Research-Atmospheres*, *118*(4), 1624-1639.

Gu, S. Y., T. Li, X. Dou, N.-N. Wang, D. Riggin, and D. Fritts (2013b), Long-term observations of the quasi two-day wave by Hawaii MF radar, *Journal of Geophysical Research: Space Physics*, *118*(12), 2013JA018858.

Guharay, A., P. P. Batista, and B. R. Clemesha (2015), Variability of the quasi-2-day wave and interaction with longer period planetary waves in the MLT at Cachoeira Paulista (22.7°S, 45°W), *Journal of Atmospheric and Solar-Terrestrial Physics*, *130–131*, 57-67.

Haynes, P. H., M. E. McIntyre, T. G. Shepherd, C. J. Marks, and K. P. Shine (1991), On the “Downward Control” of Extratropical Diabatic Circulations by Eddy-Induced Mean Zonal Forces, Journal of the Atmospheric Sciences, 48(4), 651-678.

Körnich, H., and E. Becker (2010), A simple model for the interhemispheric coupling of the middle atmosphere circulation, *Advances in Space Research*, *45*(5), 661-668.

Karlsson, B., H. Körnich, and J. Gumbel (2007), Evidence for interhemispheric stratosphere-mesosphere coupling derived from noctilucent cloud properties, *Geophysical Research Letters*, *34*(16), L16806.

Karlsson, B., C. McLandress, and T. G. Shepherd (2009), Inter-hemispheric mesospheric coupling in a comprehensive middle atmosphere model, *Journal of Atmospheric and Solar-Terrestrial Physics*, *71*(3–4), 518-530.

Lieberman, R. S., D. M. Riggin, D. A. Ortland, J. Oberheide, and D. E. Siskind (2015), Global observations and modeling of nonmigrating diurnal tides generated by tide-planetary wave interactions, *Journal of Geophysical Research: Atmospheres*, *120*(22), 11,419-411,437.

Lilienthal, F., and C. Jacobi (2015), Meteor radar quasi 2-day wave observations over 10 years at Collm (51.3° N, 13.0° E), *Atmos. Chem. Phys.*, *15*(17), 9917-9927.

Lima, L. M., E. O. Alves, P. P. Batista, B. R. Clemesha, A. F. Medeiros, and R. A. Buriti (2012), Sudden stratospheric warming effects on the mesospheric tides and 2-day wave dynamics at 7°S, J. Atmos. Sol. Terr. Phys., 78–79, 99–107, doi:10.1016/j.jastp.2011.02.013.

Limpasuvan, V., and D. L. Wu (2003), Two-day wave observations of UARS Microwave Limb Sounder mesospheric water vapor and temperature, *Journal of Geophysical Research-Atmospheres*, *108*(D10), -.

Limpasuvan, V., and D. L. Wu (2009), Anomalous two-day wave behavior during the 2006 austral summer, *Geophys. Res. Lett.*, *36*(4), L04807.

Liu, H. L., and R. G. Roble (2002), A study of a self-generated stratospheric sudden warming and its mesospheric-lower thermospheric impacts using the coupled TIME-GCM/CCM3, *J. Geophys. Res.*, *107*(D23), 4695.

Liu, H. L., E. R. Talaat, R. G. Roble, R. S. Lieberman, D. M. Riggin, and J. H. Yee (2004), The 6.5-day wave and its seasonal variability in the middle and upper atmosphere, *J. Geophys. Res.*, *109*(D21), D21112.

Lossow, S., C. McLandress, A. I. Jonsson, and T. G. Shepherd (2012), Influence of the Antarctic ozone hole on the polar mesopause region as simulated by the Canadian Middle Atmosphere Model, Journal of Atmospheric and Solar-Terrestrial Physics, 74, 111-123.

Lubis, S. W., N. E. Omrani, K. Matthes, and S. Wahl (2016), Impact of the Antarctic Ozone Hole on the Vertical Coupling of the Stratosphere-Mesosphere-Lower Thermosphere System, Journal of the Atmospheric Sciences, 73(6), 2509-2528.

Madhavi, G. N., P. Kishore, S. V. B. Rao, I. Velicogna, and G. Basha (2015), Two-day wave observations over the middle and high latitudes in the NH and SH using COSMIC GPSRO measurements, *Advances in Space Research*, *55*(2), 722-731.

Matsuno, T. (1971), A Dynamical Model of the Stratospheric Sudden Warming, *Journal of the Atmospheric Sciences*, *28*(8), 1479-1494.

McCormack, J. P., L. Coy, and K. W. Hoppel (2009), Evolution of the quasi 2-day wave during January 2006, *J. Geophys. Res.*, *114*(D20), D20115.

McCormack, J. P., L. Coy, and W. Singer (2014), Intraseasonal and interannual variability of the quasi 2 day wave in the Northern Hemisphere summer mesosphere, *Journal of Geophysical Research: Atmospheres*, *119*(6), 2928-2946.

McCormack, J. P., S. D. Eckermann, K. W. Hoppel, and R. A. Vincent (2010), Amplification of the quasi-two day wave through nonlinear interaction with the migrating diurnal tide, *Geophys. Res. Lett.*, *37*(16), L16810.

Palo, S. E., J. M. Forbes, X. Zhang, J. M. Russell III, and M. G. Mlynczak (2007), An eastward propagating two-day wave: Evidence for nonlinearplanetary wave and tidal coupling in the mesosphere and lower thermosphere, Geophys. Res. Lett., 34, L07807, doi:10.1029/2006GL027728.

Pancheva, D., P. Mukhtarov, D. E. Siskind, and A. K. Smith (2016), Global distribution and variability of quasi 2 day waves based on the NOGAPS-ALPHA reanalysis model, *Journal of Geophysical Research: Space Physics*, n/a-n/a.

Pancheva, D. M., N. J.; Manson, A. H.; Meek, C. E.; Jacobi, Ch.; Portnyagin, Yu.; Merzlyakov, E.; Hocking, W. K.; MacDougall, J.; Singer, W.; Igarashi, K.; Clark, R. R.; Riggin, D. M.; Franke, S. J.; Kürschner, D.; Fahrutdinova, A. N.; Stepanov, A. M.; Kashcheyev, B. L.; Oleynikov, A. N.; Muller, H. G. (2004), Variability of the quasi-2-day wave observed in the MLT region during the PSMOS campaign of June-August 1999, *Journal of Atmospheric and Solar-Terrestrial Physics*, *66*(6-9), 539-565.

Pedatella, N. M., and J. M. Forbes (2012), The quasi 2 day wave and spatial-temporal variability of the OH emission and ionosphere, *J. Geophys. Res.*, *117*(A1), A01320.

Sandford, D. J., M. J. Schwartz, and N. J. Mitchell (2008), The wintertime two-day wave in the polar stratosphere, mesosphere and lower thermosphere, Atmos. Chem. Phys., 8(3), 749–755, doi:10.5194/acp-8-749-2008.

Schwartz, M.J., Lambert, A., Manney, G.L., et al., 2008. Validation of the Aura microwave limb sounder temperature and geopotential height measurements. J. Geophys. Res. 113, D15S11. http://dx.doi.org/10.1029/2007JD008783.

Siskind, D. E., and J. P. McCormack (2014), Summer mesospheric warmings and the quasi 2 day wave, *Geophysical Research Letters*, 2013GL058875.

Siskind, D. E., D. P. Drob, J. T. Emmert, M. H. Stevens, P. E. Sheese, E. J. Llewellyn, M. E. Hervig, R. Niciejewski, and A. J. Kochenash (2012), Linkages between the cold summer mesopause and thermospheric zonal mean circulation, *Geophysical Research Letters*, *39*(1).

Stray, N. H., Y. J. Orsolini, P. J. Espy, V. Limpasuvan, and R. E. Hibbins (2015), Observations of planetary waves in the mesosphere-lower thermosphere during stratospheric warming events, *Atmos. Chem. Phys.*, *15*(9), 4997-5005.

Tan, B., X. Chu, H.-L. Liu, C. Yamashita, and J. M. Russell, III (2012), Zonal-mean global teleconnection from 15 to 110 km derived from SABER and WACCM, *J. Geophys. Res.*, *117*(D10), D10106.

Tunbridge, V. M., D. J. Sandford, and N. J. Mitchell (2011), Zonal wave numbers of the summertime 2 day planetary wave observed in the mesosphere by EOS Aura Microwave Limb Sounder, *J. Geophys. Res.*, *116*(D11), D11103.

Wang, J. C., L. C. Chang, J. Yue, W. Wang, and D. E. Siskind (2017), The quasi 2 day wave response in TIME-GCM nudged with NOGAPS-ALPHA, *Journal of Geophysical Research: Space Physics*, 122, doi:10.1002/2016JA023745.

Yue, J., H.-L. Liu, and L. C. Chang (2012), Numerical investigation of the quasi 2 day wave in the mesosphere and lower thermosphere, *J. Geophys. Res.*, *117*(D5), D05111.

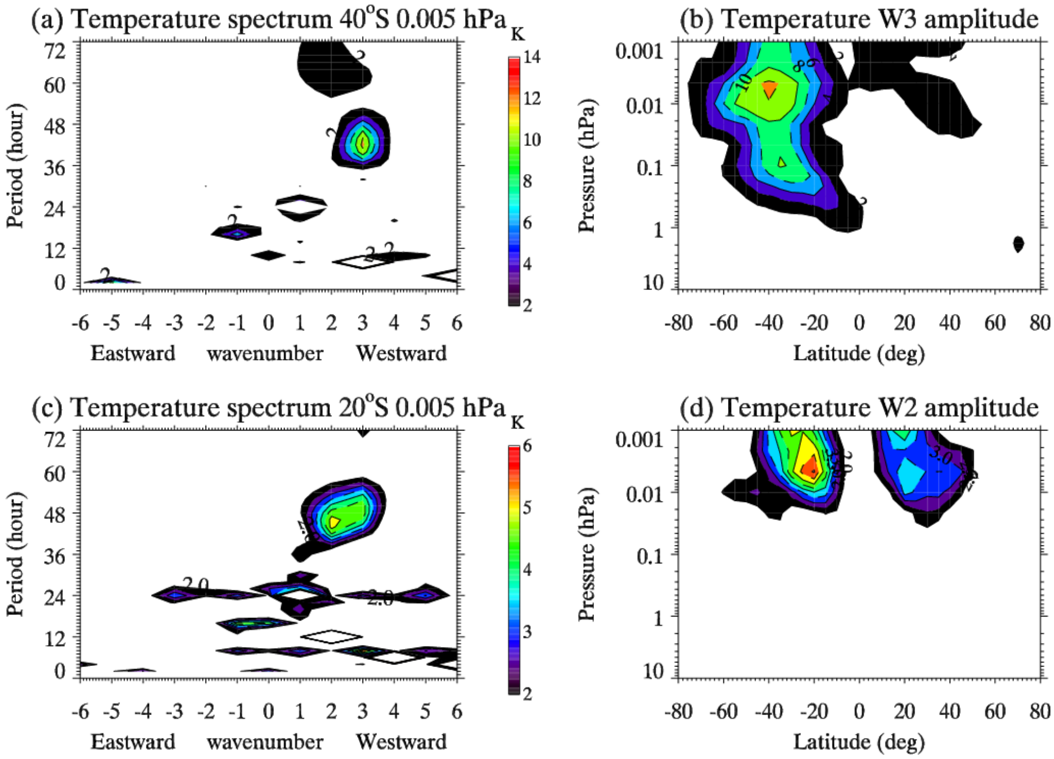

Figure 1 The wave number-period spectra of the Aura/MLS temperature observations during (a) January 12-19 of 2006 at ~40°S and ~0.005 hPa, (c) January 23-30 of 2006 at ~20°S and ~0.005 hPa. The corresponding latitudinal and vertical structures of the W3 and W2 QTDWs are shown in (b) and (d), respectively.

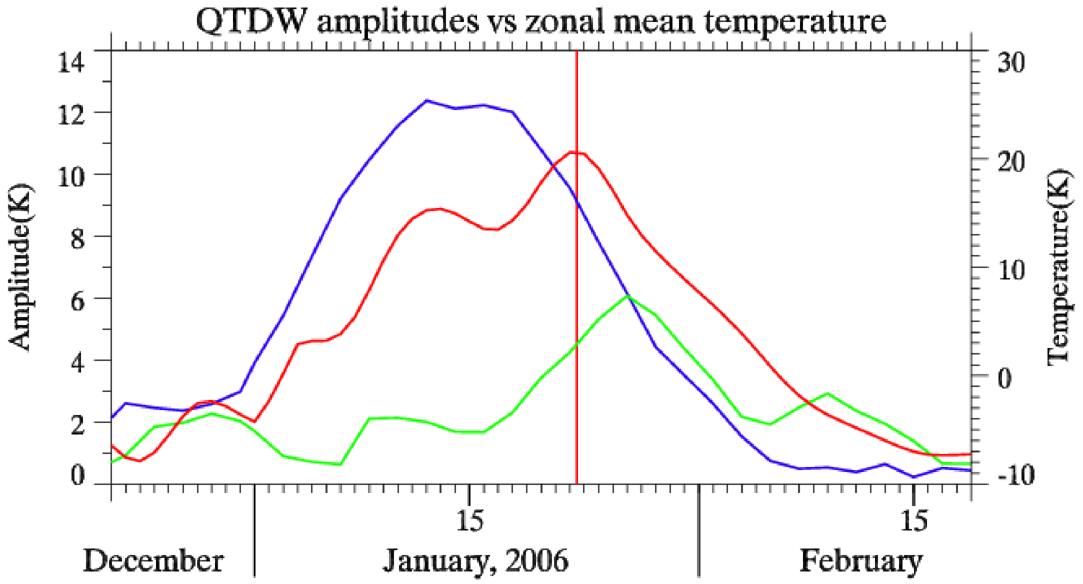

Figure 2 The temporal variations of the (blue) W3 at ~40°S and (green) W2 at ~20°S. The zonal mean temperature deviations from seasonal (90-day) mean at 70°N and 10 hPa is also plotted (red). The Aura/MLS temperature observations are utilized in the analysis. The vertical red line indicates the warming peak of the SSW.

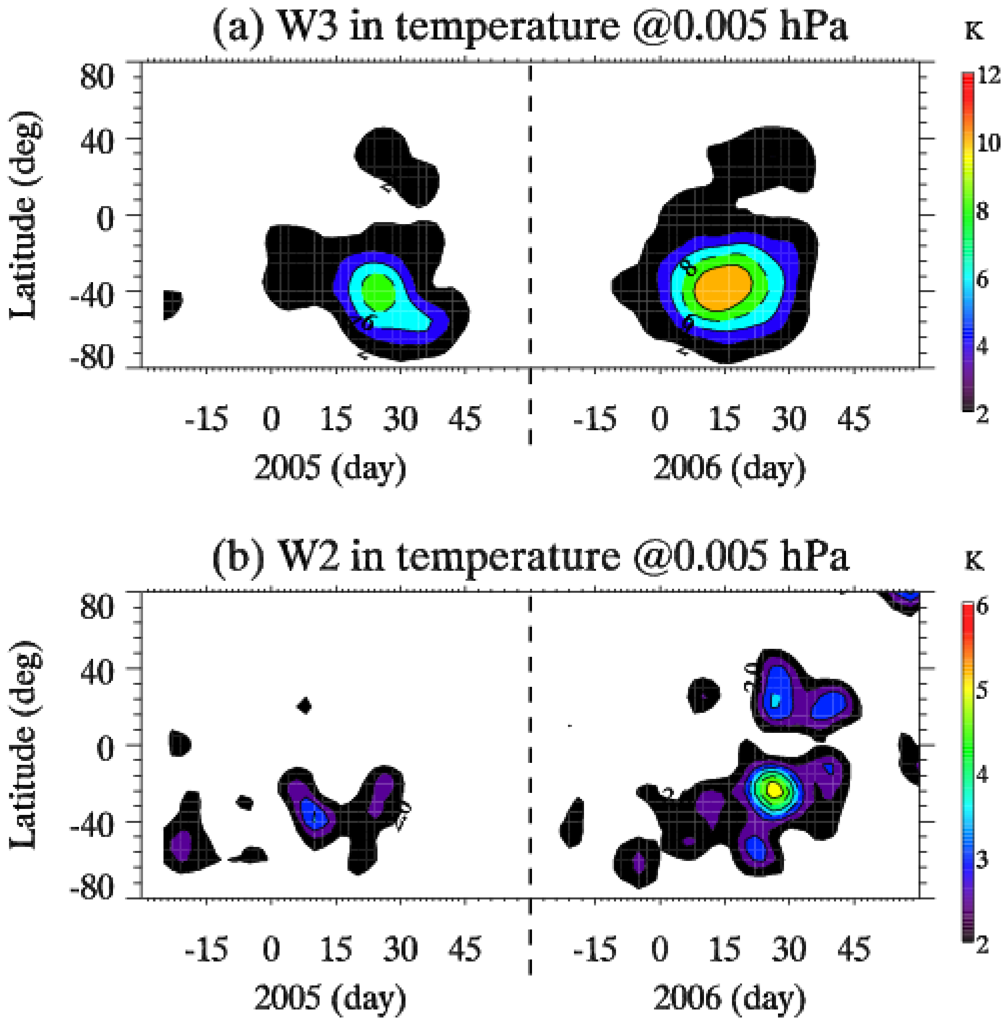

Figure 3 Temporal variations of the (a) W3 and (b) W2 in Aura/MLS temperature observations at ~0.005 hPa during 2005 and 2006.

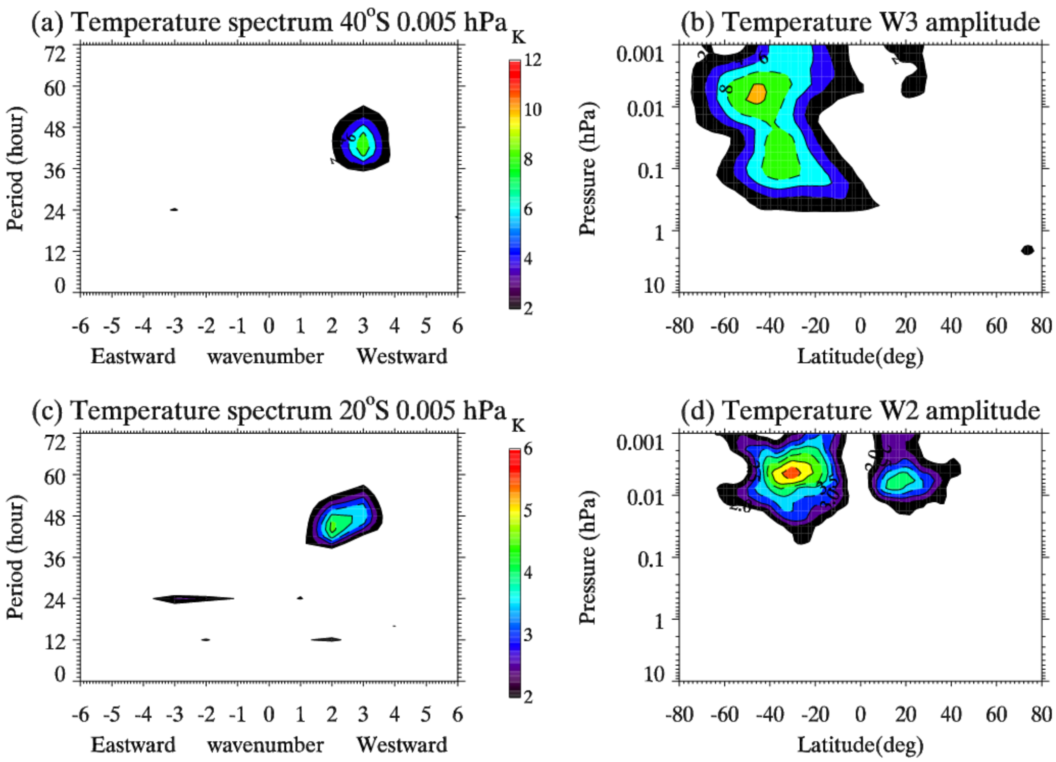

Figure 4 The same as Figure 1 but for the NOGAPS-ALPHA reanalysis datasets.

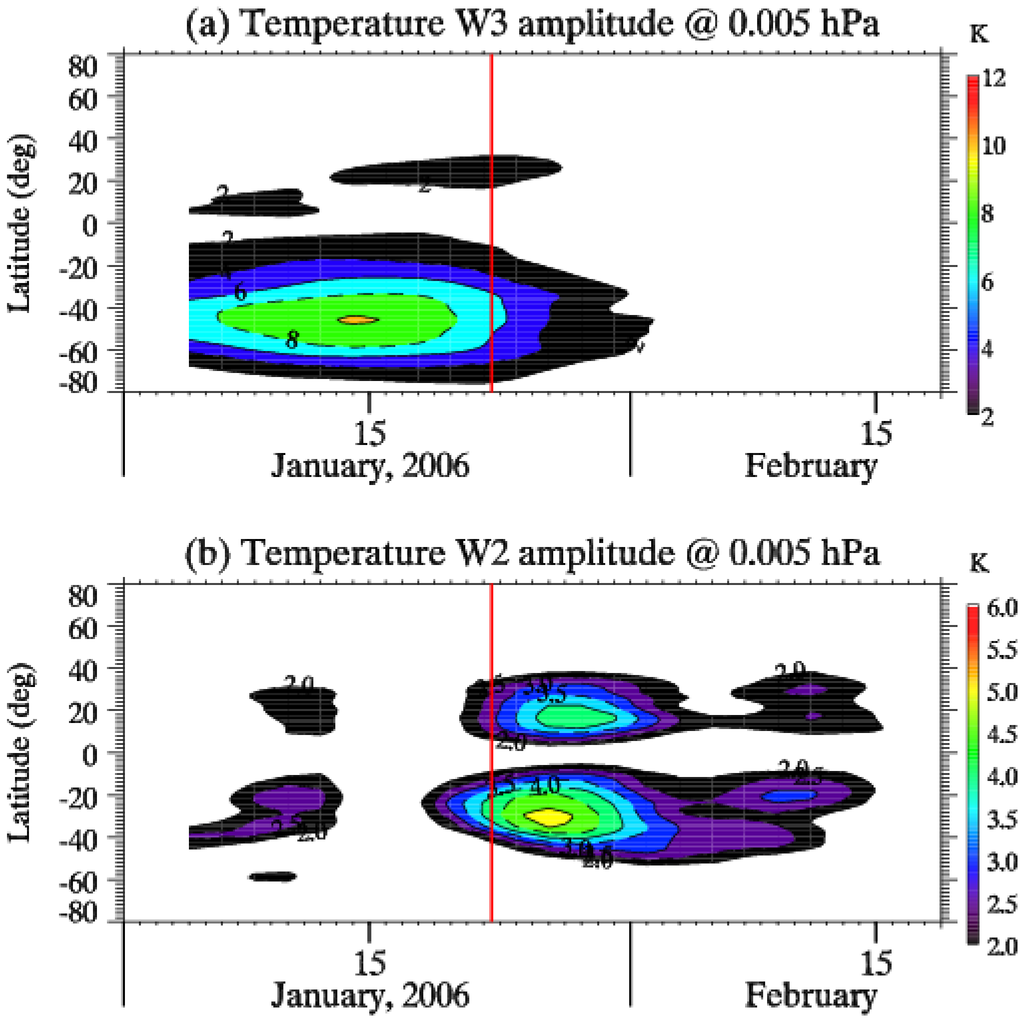

Figure 5 Temporal variations of the (a) W3 and (b) W2 QTDWs at ~0.005 hPa during 2006 from NOGAPS-ALPHA reanalysis dataset. The vertical red lines indicate the warming peak of SSW.

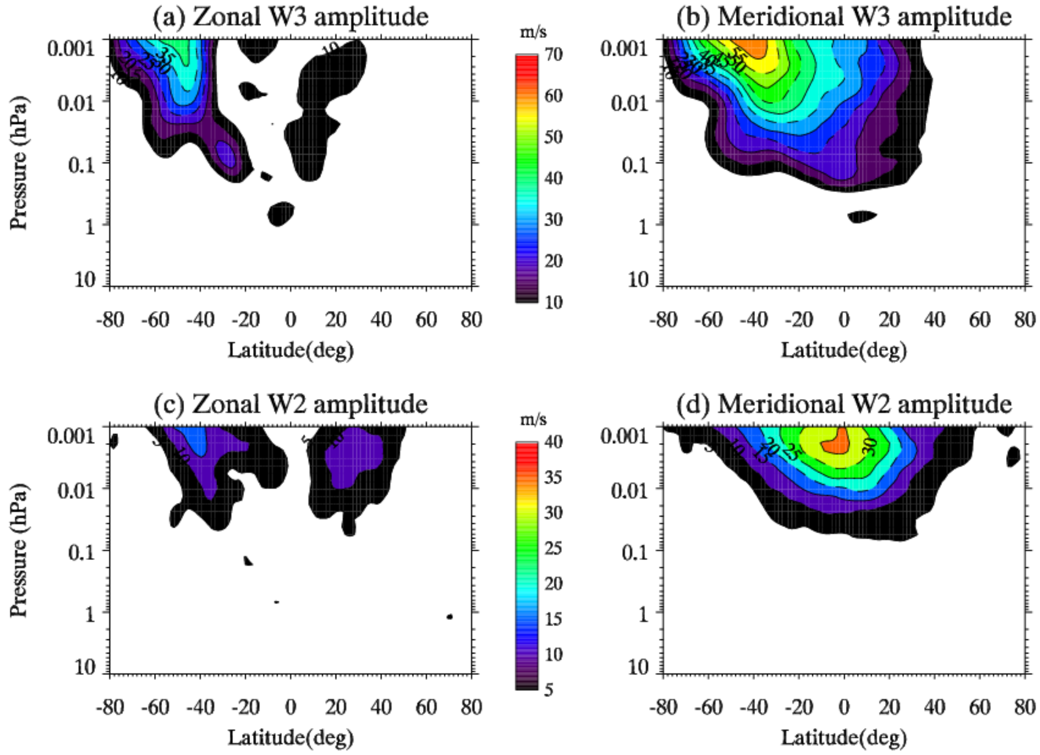

Figure 6 Altitude-latitude structures of the (a, b) W3 and (b, d) W2 in (a, c) zonal and (b, d) meridional wind components. The wind fields during January 12-19 and 23-30 of 2006 are utilized for the analysis of W3 and W2, respectively.

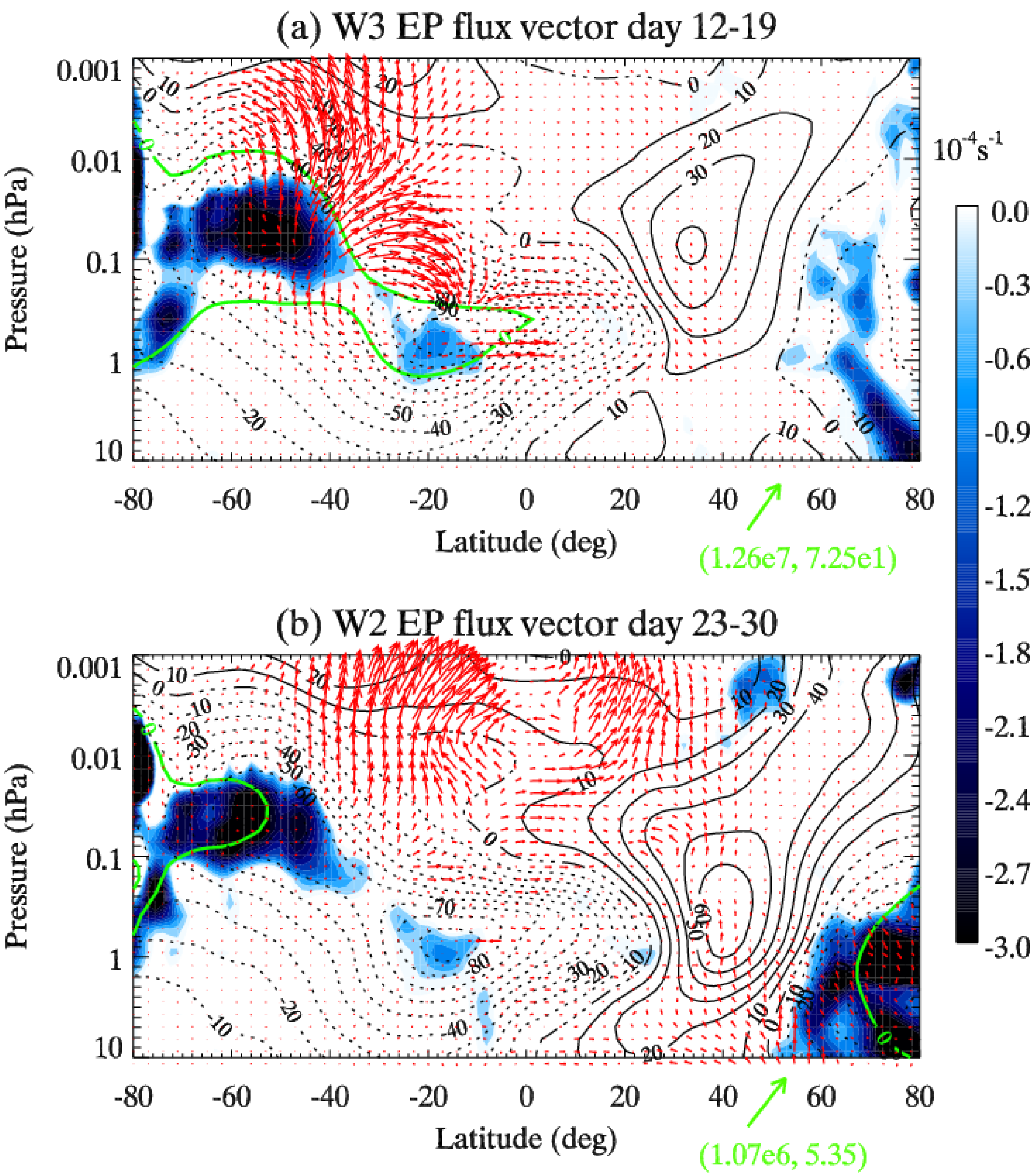

Figure 7 The EP flux vectors of (a) W3 during January 12-19 and (b) W2 during January 23-30. The barotropically/baroclinically unstable regions ($\bar{q}_{\varphi} < 0$, equation 1) are shaded with blue, and the critical layers are overplotted with green lines. The EP flux vectors are normalized by the square root of the neutral density. The reference lengths are shown at right bottom.

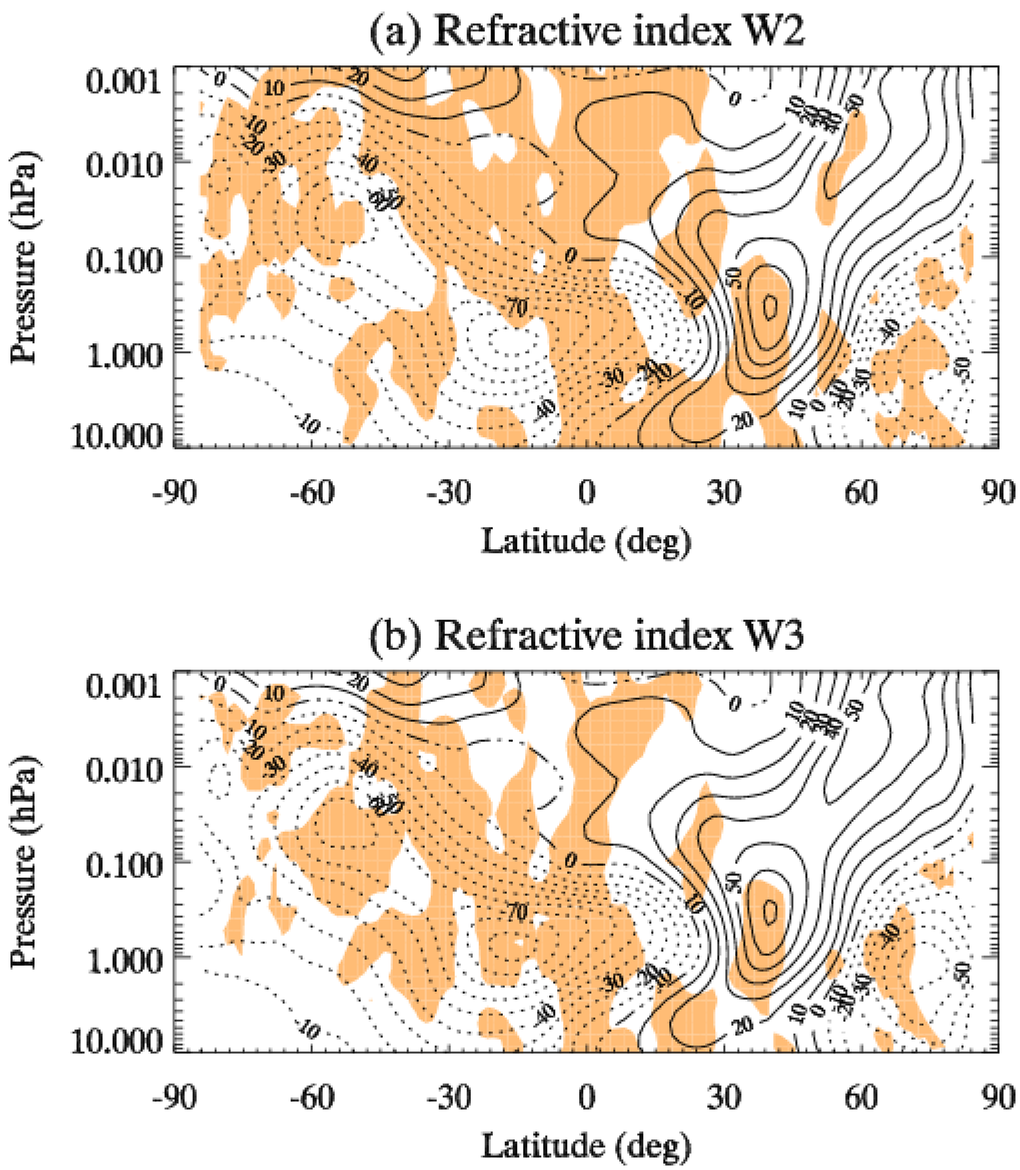

Figure 8 The refractive index (waveguide) of W2 and W3. The zonal mean zonal wind during January 10-30 is utilized in the analysis. The shaded regions indicate where the propagation of W2 or W3 is favored.

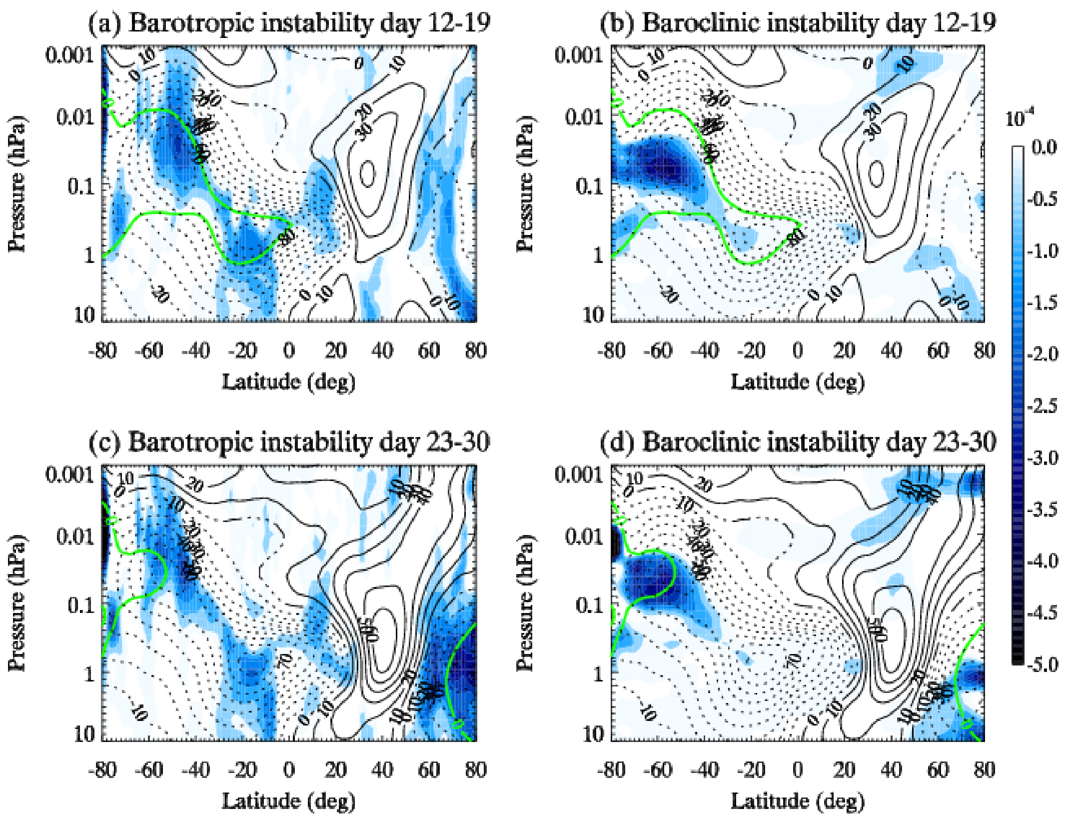

Figure 9 The (a, c) baotropic and (b, d) baroclinic instabilities during (a, b) January 12-19 and (b, d) 23-30. The blue shaded region indicates the negative values of part 2 and part 3 in equation (1). The green line in 9a and 9b (9c and 9d) shows the critical level of W3 (W2).

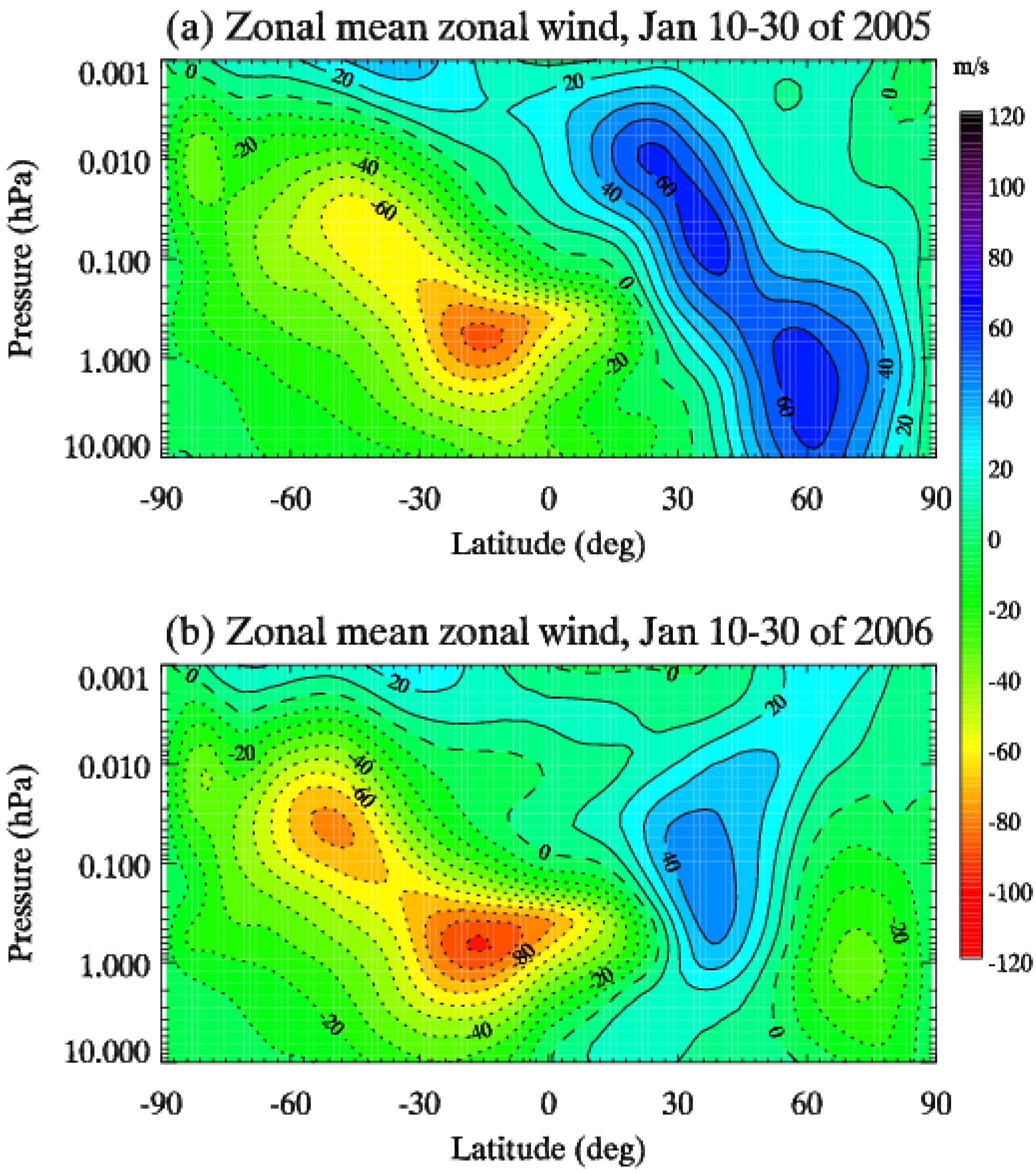

Figure ~~8~~ 10 The zonal mean zonal wind during days 10-30 of (a) 2005 and (b) 2006. The eastward and westward winds are plotted with solid and dotted lines, respectively.

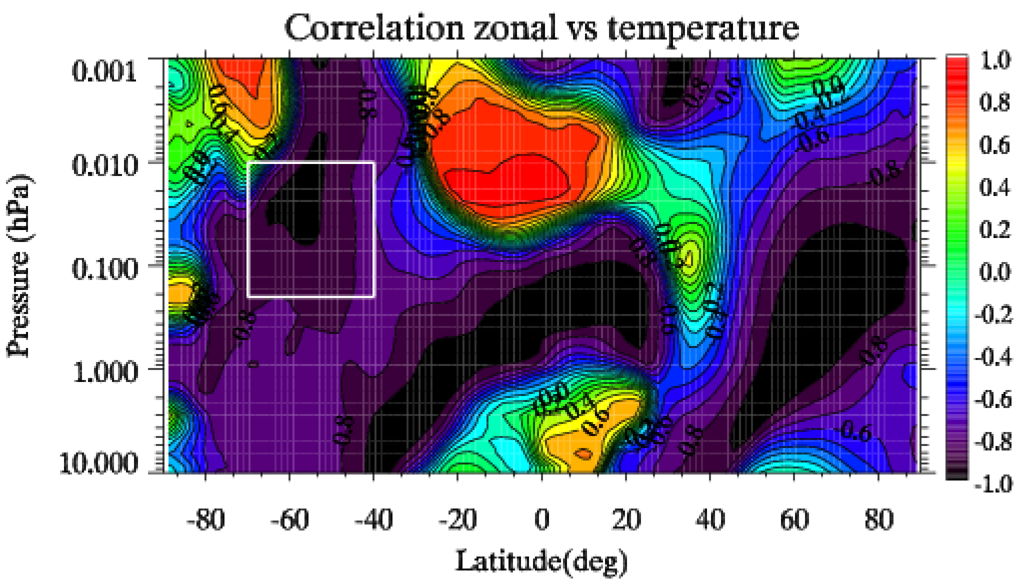

Figure ~~9~~ 11 The correlation coefficient between the global zonal mean zonal wind and the temperature at 10 hPa and 70ºN from January 1 to February 20 of 2006. The rectangle indicates the unstable region that contributes most significantly to the amplification of QTDW.

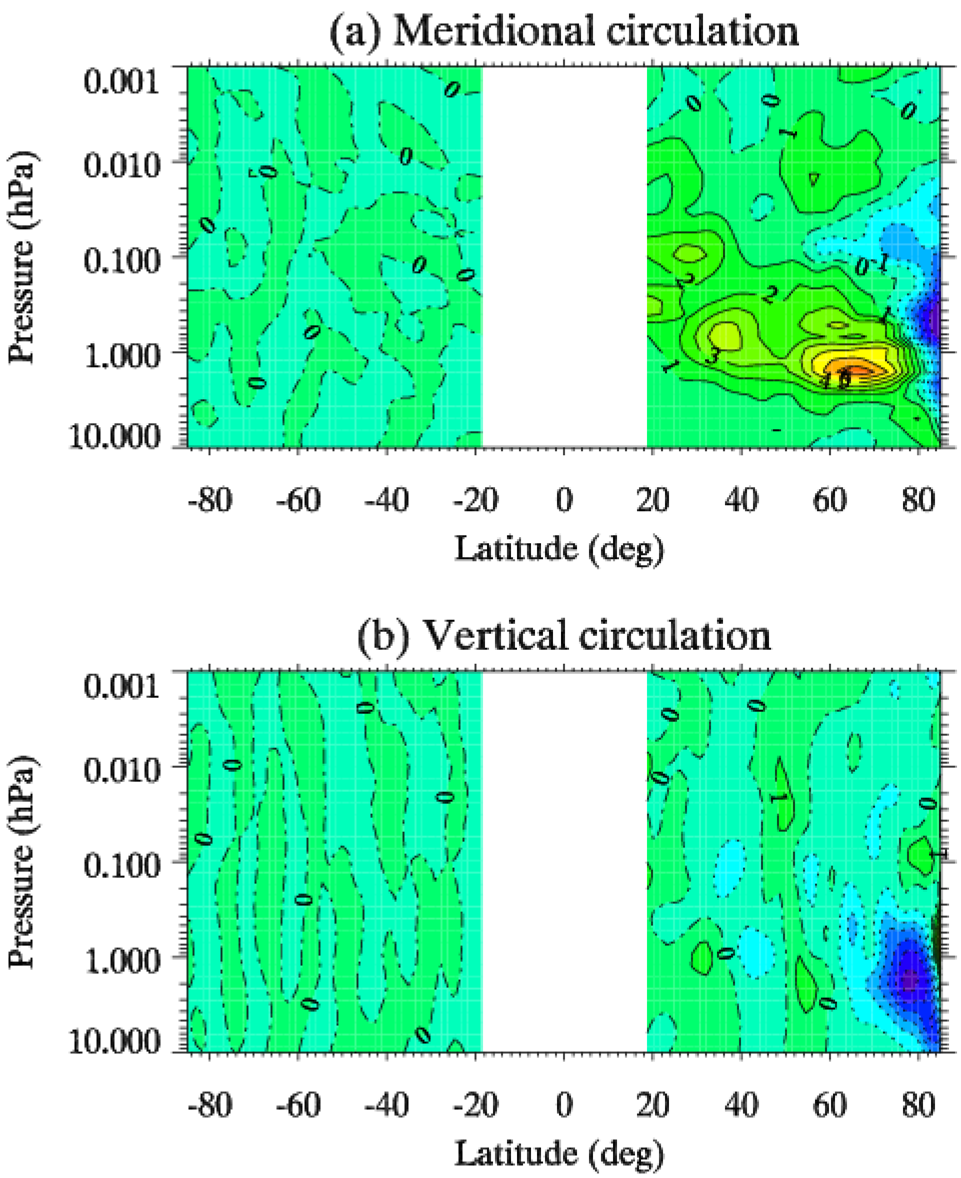

Figure 12 The (a) meridional and (b) vertical circulations induced by wave number 1 stationary planetary wave. The dataset during January 6-10, when SPW1 reaches maximum amplitude, are utilized in the analysis to show the strongest SPW1 induced variations in the zonal mean circulation. The contour intervals are 1 m/s and 1 cm/s for (a) and (b), respectively.

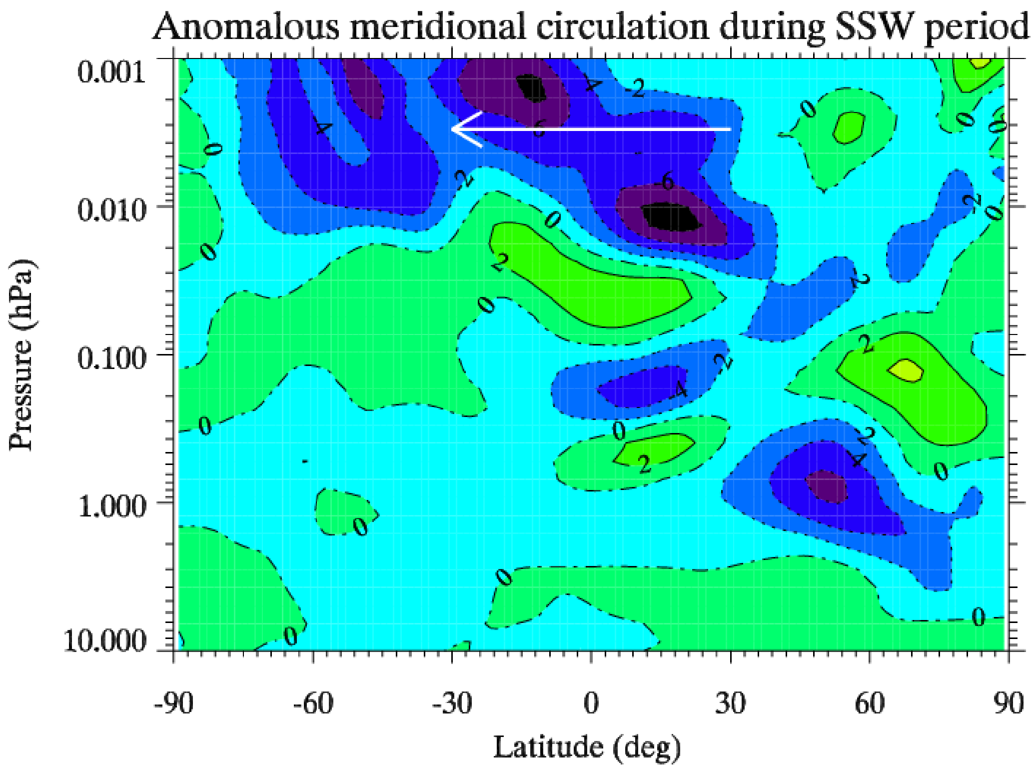

Figure 13 The differences between the total meridional circulation during and before the SSW period. The contour interval is 2 m/s.

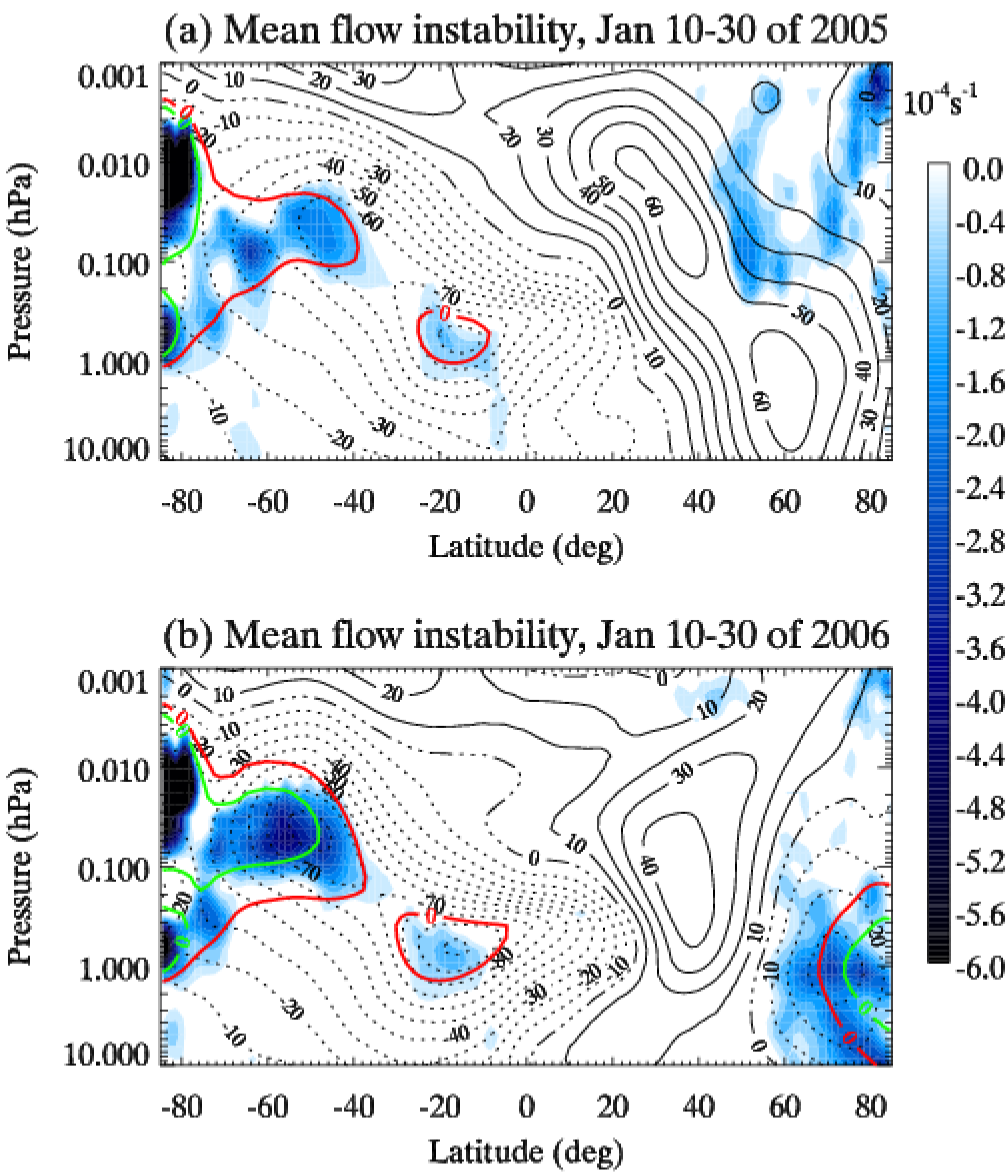

Figure ~~10~~ 14 Comparison between the critical lines of the (red) 42-hour W3 and (light green) 45-hour W2 for zonal mean zonal wind during days 10-30 of (a) 2005 and (b) 2006. The westward (eastward) zonal wind is plotted with dot (solid) lines, and the barotropically/baroclinically unstable regions ($\bar{q}_{\varphi} < 0$, equation 1) are shaded with blue.

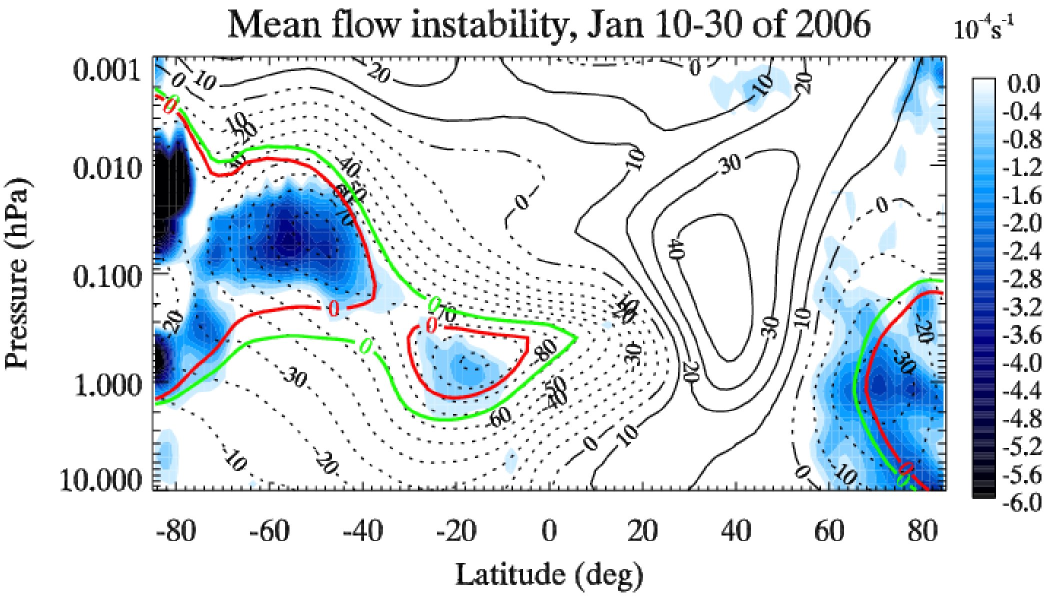

Figure ~~11~~ 15 The same as Figure 10 but for the comparison between the critical lines of the (red) 42-hour and (light green) 52-hour W3 QTDW during days 10-30 of 2006.

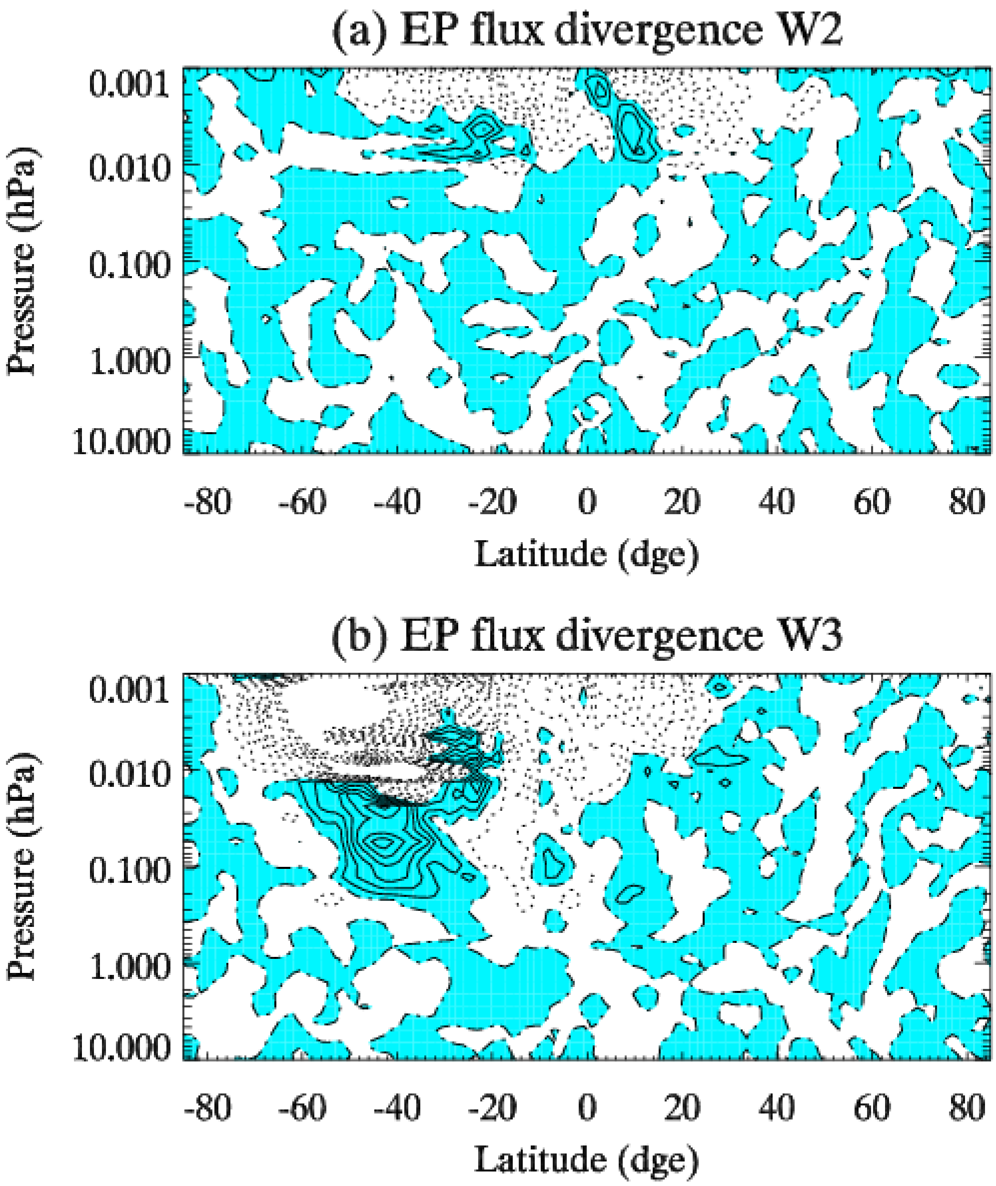

Figure ~~12~~ 16 The EP flux divergence of (a) W2 and (b) W3 during January 23-30 of 2006. The shaded region indicates positive EP flux divergence, and the contour interval is 2 m/s/day.

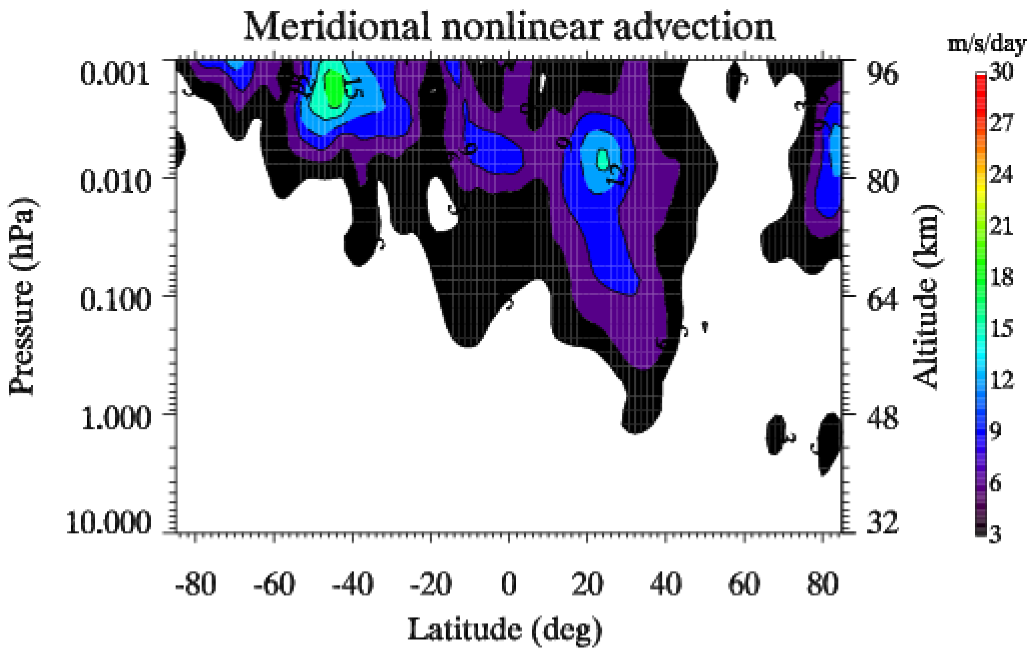

Figure ~~13~~ 17 Meridional component of the nonlinear advection between W3 and SPW1 during January 23-30 of 2006.

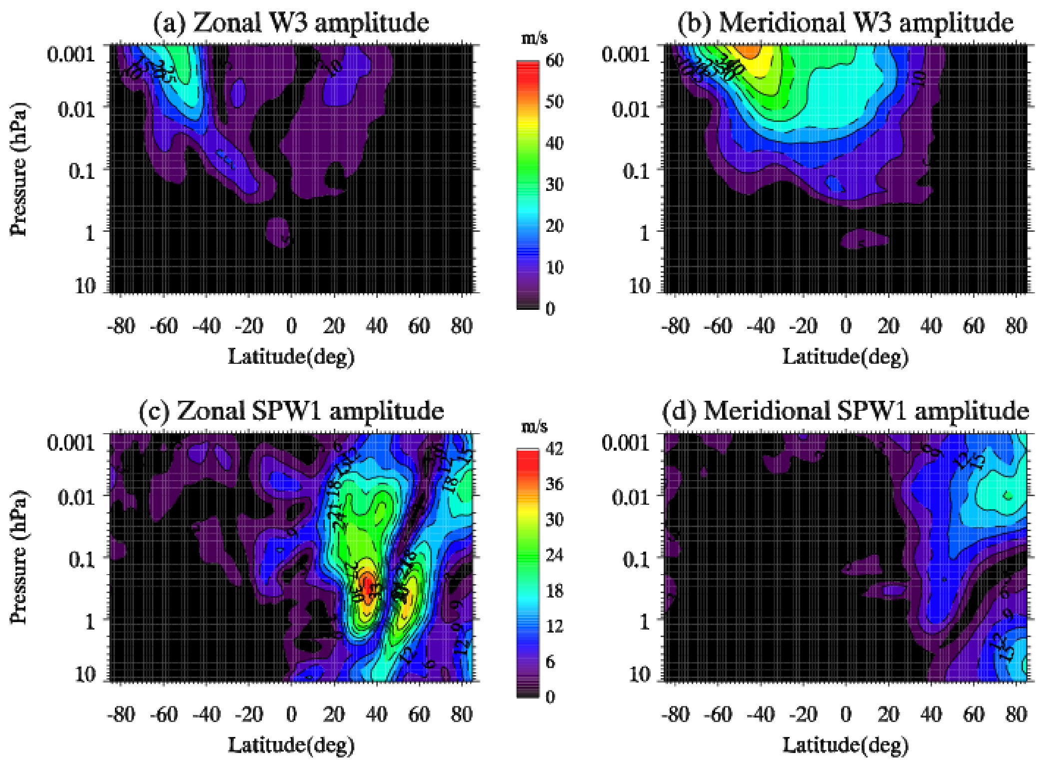

Figure ~~14~~18~~.~~ Altitude-latitude structures of (a, b) W3 and (c, d) SPW1 in (a, c) zonal and (b, d) meridional winds during January 23-30 of 2006.

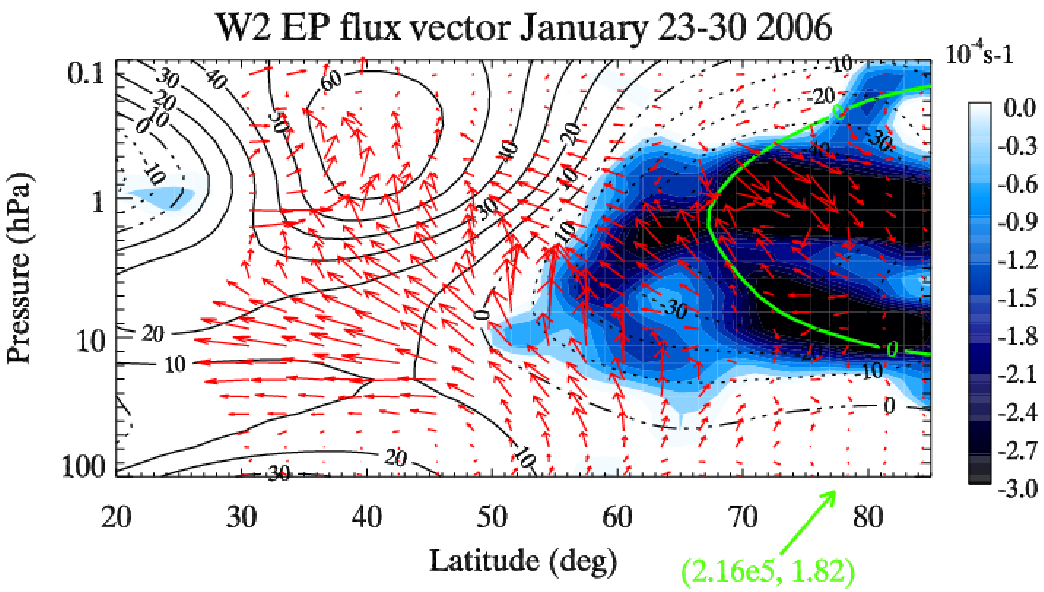

Figure ~~15~~19~~.~~ The EP flux vectors of W2 and the mean flow instabilities during January 23-30 near the winter stratosphere. The EP flux vectors are normalized by the square root of the neutral density. The reference length is shown at right bottom.